Journal of Hazardous Materials 480 (2024) 135929

Contents lists available at ScienceDirect

Journal of Hazardous Materials

journal homepage: www.elsevier.com/locate/jhazmat

Dual C and Cl compound-specific isotope analysis and metagenomic insights into the degradation of the pesticide methoxychlor

Martí Vinyes-Nadal [a,*], Steffen Kümmel [b], Yolanda Espín [c], Juan José Gómez-Alday [c], Matthias Gehre [b], Neus Otero [a,d], Clara Torrentó [a,d]

[a] Grup MAiMA, SGR Mineralogia Aplicada, Geoquímica i Hidrogeologia (MAGH), Departament de Mineralogia, Petrologia i Geologia Aplicada, Facultat de Ciències de la Terra, Institut de Recerca de l'Aigua (IdRA), Universitat de Barcelona (UB), Martí i Franquès s/n, 08028 Barcelona, Spain
[b] Department of Technical Biogeochemistry, Helmholtz Centre for Environmental Research – UFZ, Permoserstraße 15, Leipzig 04318, Germany
[c] Group of Hydrogeology, Biotechnology and Natural Resources Laboratory, Institute for Regional Development (IDR), University of Castilla-La Mancha (UCLM), 02071 Albacete, Spain
[d] Serra Húnter Fellowship, Generalitat de Catalunya, Spain

HIGHLIGHTS

- First reported C and Cl isotope fractionations for methoxychlor degradation processes.
- Dual isotope pattern was obtained for biotic methoxychlor reductive dechlorination.
- Hydrolysis and oxidation do not cause significant C and Cl isotope fractionation.
- Degradation mechanisms were postulated based on C and Cl isotope fractionations.
- Potential families involved in methoxychlor anaerobic biodegradation were identified.

GRAPHICAL ABSTRACT

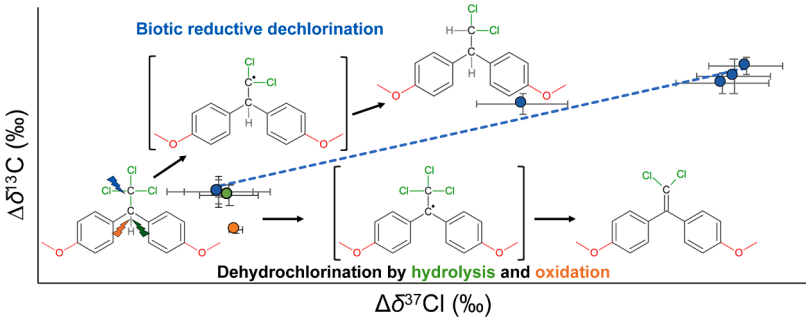

ARTICLE INFO

Keywords:
CSIA
Degradation mechanisms
Metagenomic
Kinetic isotope effect

ABSTRACT

This study investigates the use of multi-element compound-specific isotope analysis (ME-CSIA) to monitor degradation processes of methoxychlor, a persistent organochlorine insecticide. Laboratory experiments examined the kinetics, release of transformation products, and carbon and chlorine isotope effects during methoxychlor degradation through alkaline hydrolysis, oxidation with alkaline-activated persulfate, and biotic reductive dechlorination. Results showed that hydrolysis and oxidation did not cause significant carbon and chlorine isotope fractionation, indicating that C-H rather than C-Cl bond cleavage was the rate-determining step. Conversely, biotic reductive dechlorination by a field-derived microcosm under strictly anoxic conditions displayed significant carbon ($\varepsilon_C = -0.9 \pm 0.3$ ‰) and chlorine ($\varepsilon_{Cl} = -1.9 \pm 1.0$ ‰) isotope fractionation. Its corresponding calculated dual isotope slope ($\Lambda_{C/Cl} = 0.4 \pm 0.1$) and apparent kinetic isotope effects ($AKIE_C = 1.014 \pm 0.005$ and $AKIE_{Cl} = 1.006 \pm 0.003$) indicate a C-Cl bond cleavage as the rate-determining step, highlighting the difference with respect to the other studied degradation mechanisms. Changes in the microbial community diversity revealed that families such as Dojkabacteria, *Anaerolineaceae*, *Dysgonomonadaceae*, *Bacteroidetes vadinHA17*, *Pseudomonadaceae*, and *Spirochaetaceae*, may be potential agents of methoxychlor reductive

* Corresponding author.
E-mail address: martivinyesnadal@ub.edu (M. Vinyes-Nadal).

https://doi.org/10.1016/j.jhazmat.2024.135929
Received 16 July 2024; Received in revised form 7 September 2024; Accepted 19 September 2024
Available online 20 September 2024

dechlorination under anoxic conditions. This study advances the understanding of degradation mechanisms of methoxychlor and improves the ability to track its transformation in contaminated environments, including for the first time an isotopic perspective.

1. Introduction

Organochlorine pesticides (OCPs) constitute a major environmental issue due to their considerable toxicity, and propensity for bioaccumulation within the food chain [1-3]. Among OCPs, the insecticide methoxychlor (MET) (1-methoxy-4-[2,2,2-trichloro-1-(4-methoxyphenyl)ethyl]benzene) was widely adopted in the 1990s primarily in animal feeds, agriculture, and gardens [4-6]. Despite its production and use have been phased out or banned in many countries since the early 2000s [7-9], several sites are still highly polluted with this compound because its relatively low solubility and high partition coefficient (Table A1) entail a high persistence in soils [10-12]. Even though MET is mainly detected in soils, it has also been found in groundwater [13,14], making its monitoring in drinking water resources fundamental. MET has been shown to potentially induce the growth of ovarian cancer cell [15] and exhibits high toxicity towards aquatic invertebrates and fish [16]. Those negative effects make it imperative improving the knowledge about the behavior, possible degradation processes, and final destination of MET in the environment.

Although laboratory studies have reported aerobic degradation processes (oxidative dehydrochlorination, oxidative O-demethylation and CN-replacement) that might have a role in MET degradation in the environment [17-20], it is accepted that reductive dechlorination is the main metabolic pathway for MET microbial degradation [21]. This biodegradation process, which mainly results in the release of DMDD (1, 1-Dichloro-2,2-bis(4-methoxyphenyl)ethane) [19,22] (Fig. A1), is considered to be carried out cometabolically by facultative anaerobic microorganisms under suitable environmental conditions. Several bacterial species have been proved to be involved: *Klebsiella pneumoniae* in an aerobic 3 % trypticase soy broth [23], *Aeromonas hydrophila*, *Enterobacter amnigenus*, *Klebsiella terrigena*, *Bacillus subtilis*, *Acinetobacter calcoaceticus*, and *Mycobacterium obuense* under slightly anaerobic conditions [24], and *Streptomyces odorifer*, *S. xiamenesis*, *S. rimosus*, and *Micromonospora saelicesensis* isolated from organochlorine-polluted soils [25,26]. Nevertheless, bacteria responsible for this degradation pathway under strictly anoxic conditions remain unknown. Gaining a better understanding of these processes or identifying the bacteria involved could help in developing bioremediation strategies for MET-contaminated aquifers.

Natural abiotic MET degradation is limited under typical environmental conditions. The slow hydrolysis rate of MET at neutral pH and typical environmental temperatures (27 °C) results in a half-life of 367 days [27]. Abiotic MET direct photodegradation might also occur, but is also a slow environmental process [20]. Therefore, in cases where biodegradation activity is limited, remediation strategies should be explored for enhancing environmental MET degradation. Besides bioremediation, abiotic processes, mainly Advanced Oxidation Processes (AOPs), have been proposed to enhance OCPs removal, in most cases for drinking water or wastewater treatment [28]. In this sense, MET has shown low reactivity for oxidation with free chlorine, monochloramine, Cl dioxide, hydrogen peroxide and permanganate [29], but moderate or high reactivity for photodegradation with UV_{254} [29], ozonation [29,30], heterogeneous photocatalysis [31] or heterogeneous Fenton-like processes [32]. However, the use of oxidants for in situ MET remediation of soil or water bodies has been barely explored so far. A good candidate for in situ MET oxidation could be persulfate (PS), which is widely used for remediation of organic pollutants-contaminated soil and groundwater due to its low cost, high stability and aqueous solubility [33]. PS activated by different methods has been extensively explored for soils and groundwater remediation of OCPs, such as hexachlorocyclohexane (HCH) isomers [34,35] or dichlorodiphenyltrichloroethane (DDT) [36,37]. To our knowledge, however, PS has not yet been evaluated for MET oxidation. This approach might be promising, assuming a similar pathway to oxidative dehydrochlorination of MET by ligninolytic enzymes [18], which results in the release of methoxychlor olefin (MET-OLEF) (1-[2,2-dichloro-1-(4-methoxyphenyl)ethenyl]-4-methoxybenzene) (Fig. A1). Similarly, HCHs oxidation with PS occurs through a dehydrochlorination pathway [34,38].

Alkaline activation of PS may also have a synergic effect of MET alkaline hydrolysis. In an alkaline environment (pH > 10), the half-life of MET is reduced, down to 5 h at pH 13 and 27 ºC, with dehydrochlorination to MET-OLEF being the main degradation pathway [27]. Alkaline hydrolysis by dehydrochlorination has also been reported for γ-HCH [39]. Therefore, the same degradation product expected for MET alkaline hydrolysis and alkaline-activated PS might compromise distinguishing both processes in remediation projects.

For the elucidation of pesticide degradation and the assessment of remediation performance, the combined monitoring of parent pesticide dissipation and detection of transformation products [40] is often insufficient to discriminate between transformation processes and non-degradative processes such as dilution, diffusion or sorption. Compound-specific stable isotope analysis (CSIA) offers a complementary line of evidence for monitoring pollutant degradation in environmental systems [41-44] since non-degradative processes typically have negligible impact on pollutant isotopic compositions, whereas degradative processes frequently cause isotopic fractionation concerning different magnitudes and elements ($^{13}C/^{12}C$, $^{15}N/^{14}N$, $^{37}Cl/^{35}Cl$) depending on the bonds cleavage positions [45-47]. Concurrent monitoring of the signatures of two or more stable isotopes, known as Multi-Element Compound-Specific Isotope Analysis (ME-CSIA), heightens precision in the comprehension of the degradation mechanisms, since it mitigates the potential masking of single-element isotope fractionation that may result from rate-limiting steps other than bond cleavage [46].

Although ME-CSIA has been explored for detecting and distinguishing OCPs degradation processes in aquatic environments [48] and in soils [49], it has not been applied to MET degradation so far. We recently developed methods for conducting carbon ($^{13}C/^{12}C$) and chlorine ($^{37}Cl/^{35}Cl$) CSIA of MET [50], and it is now essential to evaluate the feasibility of ME-CSIA in monitoring and distinguishing the natural and induced transformation processes that MET may undergo. This approach may also facilitate a more comprehensive understanding of the mechanisms involved in MET transformation processes.

The previously discussed MET transformation pathways involve the rupture of C–Cl bonds, suggesting potential alterations in C and Cl isotope values. However, the MET molecule contains fifteen other C atoms in nonreactive positions, which could potentially dilute any C isotope ratio changes occurring at the reactive site, rendering them undetectable in some cases. In contrast, Cl isotopic analysis of MET is more promising, as the molecule contains only three Cl atoms, and isotope fractionation for this element is expected to be less affected by dilution effects. Therefore, greater compound-average isotope fractionation is anticipated for Cl compared to C [45,41,51,52]. Even with the occurrence of C isotope dilution effect of the non-reactive positions in compounds with large molecular size, measurable C isotope effects have been previously detected during transformation of OCPs and chlorinated pesticides with a high number of C atoms, such as HCH isomers, chlordecone, triazines and chloroacetamides [48,49]. ME-CSIA (C and Cl) has also demonstrated its usefulness for in-depth mechanistic interpretation during pesticide transformation by biotic and abiotic reductive

dechlorination and dehydrochlorination, and a high Cl isotope effect has also been reported for polychlorinated molecules. Indeed, detectable C and Cl isotope fractionation has been reported for biotic reductive dechlorination (Badea et al., 2009), abiotic [39] and enzymatic [53] dehydrochlorination of HCH isomers. However, ME-CSIA (C and Cl) has not yet been applied for the oxidation of polychlorinated pesticides with activated PS.

Therefore, this study evaluates the feasibility of C and Cl ME-CSIA techniques in discerning among different natural and induced transformation processes of MET. The objectives of this research are threefold: (1) to assess the degradation of MET through oxidation with alkaline-activated PS, (2) to investigate potential C and Cl isotope fractionation during MET degradation via three distinct processes involving C-Cl bonds: alkaline hydrolysis, oxidation with alkaline-activated PS, and biotic reductive dechlorination, and (3) to gain more knowledge in MET-dechlorinating microbial communities in aquifers.

2. Materials and methods

2.1. Chemicals and materials

Analytical standards MET (1-methoxy-4-[2,2,2-trichloro-1-(4-methoxyphenyl)ethyl]benzene, Pestanal® quality) and MET-OLEF (1-[2,2-dichloro-1-(4-methoxyphenyl)ethenyl]-4-methoxybenzene, standard quality) were purchased from Supelco®. These standards were used for concentration analysis, as in-house working isotope standards and to spike the experiments. Stock solutions were prepared in hexane at 1 mg/mL and stored at −18 °C.

For the extraction procedures, a DOA-P504-BN model Gast vacuum pump, a 12 port 5982–9110 model Agilent VacElut Cartridge Manifold and an IEC CL31R Multispeed ThermoFisher Scientific centrifuge were used. Cartridges used for Solid Phase Extraction (SPE) were purchased from Waters and the solvents used: hexane, dichloromethane (DCM), and ethyl acetate (EtAc), in SupraSolv® quality, and acetone and methanol (MeOH), in EMPROVE®ESSENTIAL quality, were purchased from Merck. Sodium hydroxide (NaOH) was acquired from PanReac AppliChem.

2.2. Experimental set-up

2.2.1. Biodegradation experiment

A uniform mixture of aquifer slurry was acquired from a MET-contaminated aquifer for the biodegradation experiment, with a ratio of 45 g of sediment per liter of water. This aquifer had been significantly polluted with chlorinated volatile organic compounds and pesticides as a result of previous activities of a chemical plant [54]. The mixture was sampled from the bottom of well S3, as identified in Rodríguez-Fernández et al. [54], which represents one of the most contaminated wells on the site, situated in a former tank where wastewater was discharged and with evidence of anaerobic biodegradation of chlorinated ethenes and methanes. The dried sediment of the slurry had a carbon and a nitrogen content of 2.632 ± 0.001 % and 0.45 ± 0.01 %, respectively, determined through elemental analysis [55].

Inside an anoxic Ar(g)-filled glovebox, 500 mL of the aquifer slurry was spiked at approximately 340 μg of MET per dry gram of sediment. To this end, groundwater from the S3 well was used, spiked with a 2 mg/mL MET solution in acetone and stirred for 4 h to allow the acetone to evaporate. 50 mL of the spiked groundwater was then added to 450 mL of slurry. The experiment commenced after a 72-hour equilibrium period, with static incubation maintained at a constant temperature of 21.8 ± 0.1 °C in darkness.

The slurry was completely homogenized prior to any aliquots (8 - 116 mL) sampling at 0, 42, 62, 84 and 118 days after the beginning of the experiment. Each aliquot was transferred into a sterile 50 mL Falcon tube under the anoxic environment, and the chemical and physical parameters (pH, Eh, conductivity, dissolved oxygen, temperature) were measured using a multiparametric probe. Water and sediment phases were separated by centrifugation (9000 rcf, 5 min, 4 °C). Due to low concentrations, water samples were only used for analyzing MET and metabolites concentration, whereas solid samples were used for both concentration and C and Cl CSIA analyses. After extracting MET and its metabolites, the solid samples were maintained at 50 °C until their weights stabilized to finally obtain the dry weights. Additional homogeneous slurry aliquots were sampled at time 0 and after 118 days and stored at −20 °C in sterile 50 mL plastic Falcon tubes for metagenomic analyses.

A killed control experiment was performed for assessing potential abiotic MET degradation or losses. 100 mL of the homogeneous aquifer slurry was sterilized with six autoclave cycles (steam at 121 °C under 1 atmosphere for 30 min) at 24 h intervals. The autoclaved slurry was spiked with MET at approximately 100 μg per dry gram of sediment. The remaining experimental conditions and sampling procedures were the same as those for the biodegradation experiment, except that the control experiment was sampled at 0, 20, 47, 62, 84 and 118 days.

2.2.2. Hydrolysis experiment

The alkaline MET hydrolysis experiment was performed in 500 mL deionized water buffered at a pH 11.0 ± 0.1 using NaOH pearls. The buffered solution was spiked with a 2 mg/mL solution of MET in acetone to a final concentration of approximately 23 μM. The experiment started after 30 min of equilibrium time for acetone evaporation and it was maintained at a constant temperature of 22.5 ± 0.1 °C under dark conditions by using an amber bottle that was continuously stirred to ensure homogeneity.

The pH of the solution was monitored with time, and appropriate volumes (3 – 270 mL) of homogeneous aliquots were sampled using a pipette at 0, 18, 49, 99, 126, 166 and 291 days after the beginning of the experiment for SPE and subsequent concentration and C and Cl CSIA analyses. Pesticide extraction was performed immediately to avoid further reactions.

2.2.3. Alkaline activated PS experiment

Duplicate PS experiments were performed at similar conditions as those for the hydrolysis experiment, except that 6.2 g of $Na_2S_2O_8$ was added after the 30 min equilibration time for initiating the experiment. The pH of the solution was monitored with time and kept to 10.8 ± 0.3 by adding NaOH pearls at appropriate intervals. Sampling (3 to 265 mL aliquots) and immediate SPE were performed at 0, 7, 18, 49, 99, 106 and 126 days, followed by pesticide concentration and C and Cl CSIA analyses.

2.3. Pesticide extraction methods

Samples were extracted using methods described previously [50]. Briefly, SPE was performed for water samples using Oasis HLB 500 mg cartridges (Waters), and liquid-solid extraction (LSE) with a mixture of water, methanol, and hexane was used for slurry samples. After extraction, the extracts were evaporated to dryness and reconstituted with appropriate volumes of hexane for GC-MS, GC-IRMS and GC-MC-ICPMS injections. For both extraction methods, efficiency and C and Cl isotope fractionation was evaluated previously [50].

2.4. DNA extraction

Total DNA extraction from the two slurry aliquots (500 mg of slurry, which corresponds to 18 g of sediment phase) from the biodegradation experiment was performed using NucleoSpin® Soil DNA isolation kit (Macherey-Nagel) following the manufacturer's protocol. DNA quality was analyzed on 1 % agarose gel electrophoresis. The DNA concentration and purity were assessed by measuring the ratio of absorbance at 260 and 280 nm using a lector Cytation 5 with the specific software Gen5 (Biotek). All DNA extracts were stored at −80 °C until further

analysis.

2.5. Analytical methods

2.5.1. Pesticide quantification

Concentrations of MET and MET-OLEF were measured by Gas Chromatography Mass Spectrometry (GC-MS) following the method described previously [50]. Briefly, a Shimadzu QP2010 single quadrupole GC-MS and a SAPIENS-X5MS column (30 m × 0.25 mm × 0.25 μm, Teknokroma) were used. The oven program was as follows: initial temperature of 60 °C for 1 min, ramp at 6 °C/min to 270 °C and ramp at 40 °C/min to 300 °C (total run time: 36.75 min) and the mass spectrometer was operated in electron ionization mode (70 eV). Selected-ion monitoring (SIM) measurements were performed and each analyte was quantified based on peak area using one quantifier and three qualifier ions (Table A2). Due to the lack of authentic standards, other transformation products were only tentatively identified after examination of mass spectra in full-scan mode and based on GC retention behavior and interpretation of EI-mass spectral patterns. Semi-quantitative determination of these transformation products was performed under the assumption that their MS response factors were the same as those for MET.

2.5.2. Kinetics

The kinetics of MET transformation were calculated using a pseudo-first-order rate model. Details about the determination of pseudo-first-order rate constants (k′) and half-life times ($t_{1/2}$) may be found in the Appendix A.

2.5.3. Phases concentration ratio ($C_{s/w}$)

In the biodegradation experiment, phase partitioning was evaluated during time by determining the sediment-water phases concentration ratio ($C_{s/w}$) of a given compound (C) at a given time (t), calculated using Eq. 1 [56]:

$$C_{s/w} = \log([C_t]_s/[C_t]_w) \quad (1)$$

where $[C_t]_s$ and $[C_t]_w$ are the concentrations of the considered compound in the sediment (μg/Kg) and water (μg/L) phases at a given time, respectively. Changes in the sediment-water phase concentration ratio of a given compound with time indicate that for this compound there is not equilibrium between the phases. Conversely, if the concentration ratio remains stable, it suggests that the compound has reached equilibrium between the sediment and water phases.

2.5.4. CSIA of pesticides

C and Cl isotope measurements of MET and MET-OLEF in the SPE and LSE extracts were performed by gas chromatography coupled with isotope ratio mass spectrometry (GC-IRMS), and by gas chromatography coupled with multiple-collector inductively coupled plasma mass spectrometry (GC-MC-ICPMS), respectively. Briefly, a Trace GC 1310 coupled to a MAT 253 Plus IRMS through a GC Isolink II and a Conflo IV interface (Thermo Fisher Scientific) was used for C-CSIA and a Trace 1310 GC coupled to a NEPTUNE MC-ICPMS (Thermo Fisher Scientific) via an AE2080 transferline (Aquitaine Electronique, France) was used for Cl isotope ratios determination. Further instrumental and methodological details, including linearity, precision, reproducibility and instrumental limits, may be found in Vinyes-Nadal et al. [50].

C and Cl isotope values are reported in per mil (‰) using the delta notation (δ) relative to the international reference standards Vienna PeeDee Belemnite (V-PDB) and Mean Ocean Chloride (SMOC), respectively:

$$\delta^h E(‰) = \left[\frac{R_E}{R_{E,std}} - 1\right] \quad (2)$$

where E is the considered element (C or Cl), h is the atomic mass of the heavy isotope (13 for C and 37 for Cl), R_E and $R_{E,std}$ are the isotope ratios of the element E ($^{13}C/^{12}C$ for C and $^{37}Cl/^{35}Cl$ for chlorine) in the sample and the corresponding reference standard, respectively.

2.5.5. Evaluation of stable isotope data

C and Cl isotopic fractionation (ε_C and ε_{Cl}) values were obtained from the slope of the linearized Rayleigh equation:

$$\ln\left(\frac{\delta^h E_t + 1}{\delta^h E_0 + 1}\right) = \varepsilon_E \cdot \ln f \quad (3)$$

where $\delta^h E_0$ and $\delta^h E_t$ are the isotope values of element E at the beginning (0) and at any given time (t) of the experiments, respectively, and f is the fraction of MET remaining at time t. Errors given for ε values correspond to the 95 % CI of the linear regression in Rayleigh plots.

Dual-element isotope fractionation patterns for the different degradation pathways were determined by the York regression method in 2D-isotope plots ($\Lambda_{C/Cl} = \Delta\delta^{13}C/\Delta\delta^{37}Cl$) incorporating the error measurement in both variables [57]. The uncertainty of $\Delta\delta$ values was calculated by error propagation. The uncertainty of Λ is reported showing the 95 % CI of the slope in the graphs.

Apparent kinetic isotope effects (AKIE) were calculated to assess the isotope effect of atoms at the reactive positions of the molecules. The AKIE calculations were performed using Eq. 4, where n is the total number of atoms of the considered element E in the target molecule, x is the number of atoms at the reactive site, and z represents the number of atoms involved in intramolecular isotopic competition [58].

$$AKIE_E = \frac{1}{1 + \left(\frac{n \cdot z}{x} \cdot \varepsilon_E\right)} \quad (4)$$

2.5.6. Mass balance and isotope mass balance

For each transformation reaction, the mass balance at a given time ($[C_{‰}]_t$), reported in %, was calculated using **Eq. A4**. For the biodegradation experiment, $[C_{‰}]_t$ was calculated in the slurry and in the sediment phase.

The isotope mass balance ($\delta^h E_{SUM,t}$) of a considered element (E) at any given time (t) was calculated as follows considering the parental compound and detected transformation products for which concentration and isotopic ratios are available for each sample:

$$\delta^h E_{SUM,t} \quad (‰) = \sum((\chi C_t \cdot \delta^h E_{C,t}) + (\chi C_{i,t} \cdot \delta^h E_{C_i,t}) + \ldots) \quad (5)$$

where χC_t (calculated following **Eq. A5**) and $\delta^h E_t$ are the mass fraction and isotope values of element E, respectively, of each compound at any given time (t). Uncertainties for both mass balance and isotope mass balance were calculated by error propagation. In the biodegradation experiment, the carbon isotopic mass balance was used to determine if the detected transformation product was further degraded. In a closed system where only one transformation pathway is occurring, $\delta^{13}C_{SUM}$ should remain constant as long as the last degradation product considered in the isotope mass balance is not further degraded [59,60].

As explained above, for transformation products for which no standards were available, concentrations were approached under the assumption that their GC-MS response was the same as that of MET.

2.5.7. Microbial community structure and diversity analysis

The composition and structure of the bacterial communities was assessed through amplicon sequencing of V3 and V4 variable regions of the 16S rRNA gene by the company Microomics Systems S.L. (Barcelona, Spain). PCR amplification was performed on DNA extracts and obtained libraries were sequenced using Illumina MiSeq (300 ×2). Raw demultiplexed forward and reverse reads were processed using QIIME2™ [61]. Trimming of 5′ adaptor, quality filtering of reads, denoising, amplicons merging and phylotype calling were performed using Dada2 [62]. Taxonomic profiles and diversity metrics were obtained after sequence data processing using a Bayesian classifier [63] trained with

SILVA database version 138 (full-length sequences of 99 % of observed operational taxonomic units, OTUs) [64]. Alpha-diversity was evaluated using the observed OTUs as an estimation of the community richness and the Margalef, Pielou's, Shannon-Wiener and Simpson indexes as quantitative measures of the species richness, and the community evenness, richness and diversity, respectively. The sequencing data of the slurry samples have been submitted in the NCBI Sequencing Read Archive (SRA) under the bio-project PRJNA1109749.

3. Results and discussion

3.1. MET biodegradation by reductive dechlorination

For both, the biodegradation experiment and the killed control experiment, comparable conditions based on chemical and physical parameters were observed during time. In both experiments, the pH (7.50 ± 0.03 and 7.5 ± 0.1, respectively), conductivity (5.3 ± 0.1 and 3.2 ± 0.7 mS/cm), and temperature (21.8 ± 0.9 and 21.3 ± 0.4 °C) remained constant with time, whereas slight variations were detected for the redox potential (−161 ± 97 and −36 ± 38 mV) and dissolved oxygen (0.1 ± 0.1 and 0.10 ± 0.03 mg/L) values (Table A3). This indicates constant conditions during time in both experiments and that strictly anoxic conditions were maintained throughout the experimental period.

MET consumption was detected with time in both the sediment and water phases of the slurry, whereas no MET dissipation occurred in the autoclaved slurry, discarding any MET degradation by abiotic processes or the involvement of heat-killed cells (Fig. 1). The only detected degradation product was DMDD, which is in accordance with the reductive dechlorination pathway [19]. MET degradation followed pseudo-first-order kinetics in both the solid and the water phase. Similar k' values were obtained for both phases, 0.027 ± 0.015 d^{-1} ($r^2 = 0.92$) for the sediment phase and 0.029 ± 0.009 d^{-1} ($r^2 = 0.95$) for the water phase (Fig. A2), resulting in half-life times of 26 ± 11 and 24 ± 7 days, respectively. These values align with those measured by Muir & Yarechewski [22] (28 days) during biodegradation of MET in lake and pond sediments under anoxic conditions.

The MET phases concentration ratio ($MET_{s/w}$) remained constant during time (average value of 3.9 ± 0.1) (Fig. A3). This indicates that phase partitioning for MET was in equilibrium with time. In contrast, the behavior of DMDD was different. An initial increment of DMDD concentration in both phases was observed, followed by a decrease in DMDD concentration in the solid phase, but an increase in the water phase (Fig. 1). Consequently, the DMDD phases concentration ratio ($DMDD_{s/w}$) decreased during time from 3.9 to 3.0 (Fig. A3), which is consistent with the higher affinity of DMDD for the water phase compared to MET (Table A1). Therefore, a lack of equilibrium between the phases occurred for DMDD by the end of the experiment. Furthermore, the total concentration of DMDD in the system (sediment + water) decreased with time (Table A4). The mass balance showed that after 118 days, the combined concentration of MET and DMDD had decreased to 30 % of the initial value (Table A4), indicating a significant decrease in the concentration of MET and DMDD in the sediment-water mixture. Although the determination of DMDD concentration values was performed under the assumption that their MS response factors were the same as those for MET, it is hypothesized a further biodegradation of DMDD and its displacement to the water phase.

3.2. MET degradation by alkaline hydrolysis

Methoxychlor consumption with time was also observed in the alkaline hydrolysis experiment (Fig. 1). The degradation of MET via alkaline hydrolysis (maintaining a constant pH of 11.0 ± 0.1 over 291 days) followed pseudo-first-order kinetics, with a rate constant of $k' = 0.014 \pm 0.004\ d^{-1}$ ($r^2 = 0.93$) (Fig. A2), corresponding to a half-life of 49 ± 15 days. The previously reported half-life of MET at pH levels between 3 and 8 is 367 days [27], and thus negligible contribution from neutral hydrolysis reactions was assumed in the current experiment. According to Wolfe et al. [27], MET hydrolysis above pH 10 is pH-dependent, with a second-order rate constant at 27 °C of 3.8×10^{-4}

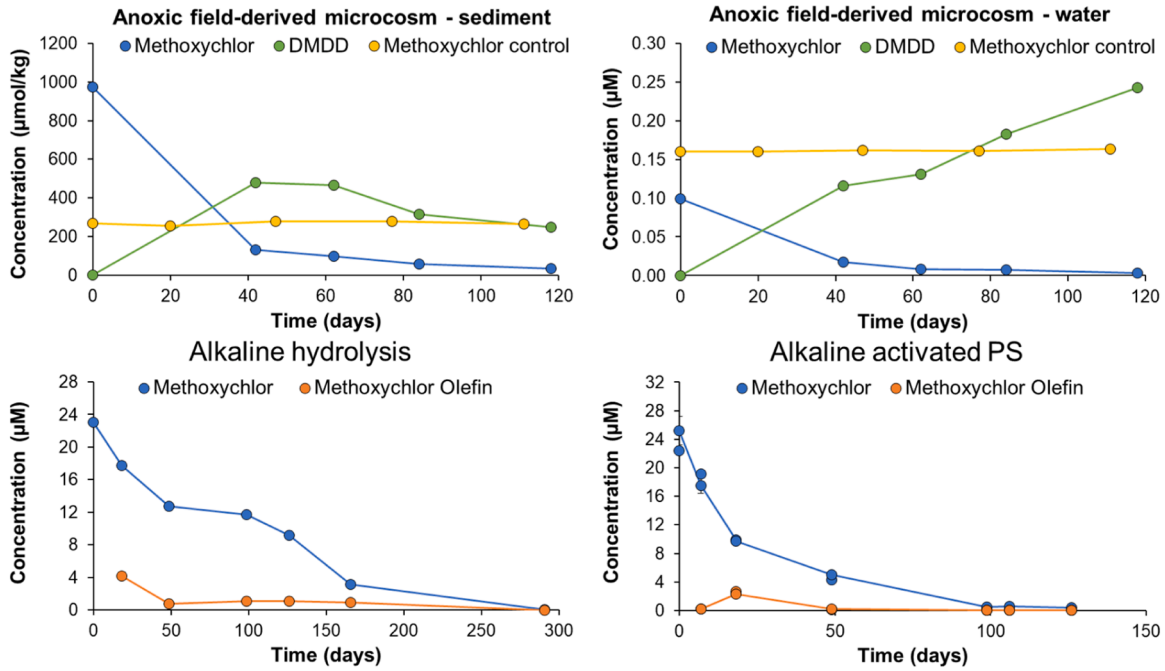

Fig. 1. Evolution with time of the concentration of MET and its detected degradation products during MET degradation by biotic reductive dechlorination and in the killed control experiment for both the sediment (upper left panel) and water (upper right panel) phases, by alkaline hydrolysis (lower left panel) and by oxidation with alkaline-activated PS (lower right panel). In the case of MET oxidation with alkaline-activated PS, the error bars stand for the standard deviation of the duplicate experiments. In most cases, error bars are smaller than the symbols. It should be noted that concentrations of DMDD were approached under the assumption that its GC-MS response was the same as that for MET (semi-quantitative determination due to the lack of standards).

M^{-1} s^{-1}. Considering this second-order rate constant, the expected MET half-life at pH 11 would be 24 days. However, in our experiment, the observed half-life was 49 days, likely due to the temperature variation between our experiment (22.5 ºC) and that conducted by Wolfe et al. [27] (27 °C). There are no empirical data available to adjust the expected kinetics to a defined temperature. More details of the results may be found in Table A5.

MET-OLEF was detected as degradation product, in accordance with the degradation pathway suggested by Wolfe et al. [27] of MET dehydrochlorination. Mass balance calculations indicated that a notable portion of MET and MET-OLEF could not be accounted of (Fig. 1), suggesting the formation of additional transformation products not examined in the current study or further transformation of MET-OLEF. No other transformation products were identified via GC-MS, although no specific efforts were undertaken to identify potential transformation products that may not be detectable by GC-MS. The change in concentration of MET-OLEF with time also suggests its further transformation (Fig. 1), likely through alkaline hydrolysis. Further investigation would be required to validate this hypothesis.

3.3. MET degradation by oxidation with alkaline-activated PS

In the alkaline-activated PS experiment, MET consumption also occurred and it exhibited pseudo-first-order kinetics with a k' value of 0.038 ± 0.006 d^{-1} ($r^2 = 0.93$) (Fig. A2), resulting in a half-life of 18 ± 3 days. Detailed data may be found in Table A6. The faster MET degradation observed in this experiment compared to the alkaline hydrolysis confirmed MET oxidation by alkaline-activated PS in addition to degradation by alkaline hydrolysis, which also occurred in this experiment due to the high pH of the solution (pH 10 ± 3). This synergic effect looks promising for the application of this approach for in situ remediation of MET-contaminated aquifers.

Our hypothesis of a degradation pathway for MET oxidation with PS similar to the oxidative dehydrochlorination by ligninolytic enzymes [18] is corroborated by the detection of MET-OLEF as a transformation product (Fig. 1). Mass balance calculations indicated that by the end of the experiment, nearly all MET would have either been mineralized or converted to other unidentified products. In fact, the change in concentration with time suggests additional transformation of MET-OLEF (Fig. 1). This aligns with the outcomes of the alkaline hydrolysis experiment, that points to transformation of MET-OLEF through alkaline hydrolysis, and with the research of Hirai et al. [18], which demonstrated that MET-OLEF is also susceptible to degradation through oxidative dehydrochlorination.

3.4. Isotopic results

Methoxychlor degradation by alkaline hydrolysis and oxidation with alkaline-activated PS resulted in non-significant ($p > 0.05$) C and Cl isotope effects (Fig. A4). In contrast, MET consumption in the biodegradation experiment was coupled to a significant enrichment in both ^{13}C ($\delta^{13}C$ from −31.8 to up to −29.0 ‰), and ^{37}Cl isotopes ($\delta^{37}Cl$ from −6.6 up to −0.8 ‰) measured from MET extracted from the sediment phase (Table A3). The C and Cl isotopic fractionation values associated to MET reductive dechlorination were determined as $\varepsilon_C = -0.9 \pm 0.3$ ‰ (R^2 =0.97) and $\varepsilon_{Cl} = -1.9 \pm 1.0$ ‰ (R^2 =0.92), respectively (Fig. A4). A $\Lambda_{C/Cl}$ value of 0.4 ± 0.1 (R^2 =0.97) was obtained from the dual C-Cl isotope plot (Fig. 2). Since this is the first study applying CSIA to MET degradation, comparison of the obtained isotopic fractionation values with previous works is not possible. As expected due to the high number of C atoms in MET, a weak C isotope fractionation was observed, but still statistically significant ($p > 0.05$). The pronounced Cl isotope effect demonstrates that Cl isotope fractionation is a particularly strong indicator of MET biodegradation.

The C isotopic composition of the produced DMDD was initially depleted in ^{13}C, in agreement with the normal isotope effect for MET degradation, and shifted toward more ^{13}C-enriched values during the reaction (from $\delta^{13}C = -32.1$ ‰ to −30.0 ‰; Fig. A5). A similar behavior was observed for $\delta^{37}Cl$ values, shifting from −9.8 ‰ to −4.7 ‰. C and Cl isotope ratios in DMDD at the end of the experiment exceeded the initial MET isotopic composition ($\delta^{13}C = -31.8$ ‰ and $\delta^{37}Cl = -6.8$ ‰). Accordingly, deviations in the isotope mass balance ($\delta^{h}E_{SUM}$) were observed for both C (with a final $\delta^{13}C_{SUM}$ value of −29.9 ± 0.1 ‰ higher than the initial $\delta^{13}C_{MET}$ value of −31.8 ± 0.2 ‰) and Cl ($\delta^{37}Cl_{SUM,f}$ of −4.2 ± 0.4 ‰ > $\delta^{37}Cl_{MET,0}$ of −6.6 ± 2.8 ‰) (Table A4). This confirms our hypothesis that DMDD was also being degraded throughout the experimental period. The low pesticide contents in the water phase hindered CSIA, preventing a further discussion about in which phase pesticide degradation prevailed. In any case, overall results point to biodegradation of both MET and DMDD, with partitioning equilibrium for MET, but DMDD preferential displacement to the water phase.

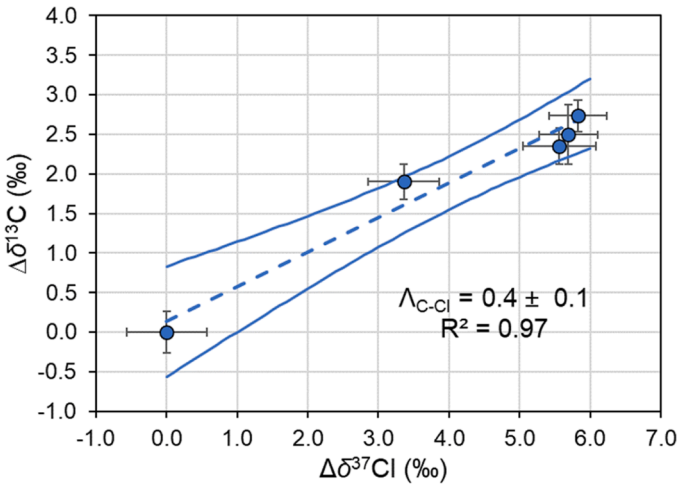

Fig. 2. Dual isotope plot ($\Delta\delta^{13}C$ vs. $\Delta\delta^{37}Cl$) for MET biotic reductive dechlorination. Error bars display the uncertainty calculated by error propagation. The slope (Λ value) was calculated by the York regression method. The uncertainty (solid lines) is shown as 95 % CI.

3.5. Degradation mechanisms

For the biodegradation experiment, the AKIEs were calculated to evaluate the reaction mechanisms (Table A7). The obtained $AKIE_C$ and $AKIE_{Cl}$ values for the reductive dechlorination of MET (1.014 ± 0.005 and 1.006 ± 0.003, respectively) are below the theoretical Streitwieser limits for the kinetic isotope effect (KIE) of a C–Cl bond cleavage, which are $KIE_C = 1.057$ and $KIE_{Cl} = 1.013$ [58]. Moreover, these values are also lower than those considered realistic for transition states at about 50 % bond cleavage ($KIE_C = 1.029$ and $KIE_{Cl} = 1.007$) [58]. This deviation from expected KIE values, known as masking effect, is thought to result from non-fractionating, rate-limiting steps that occur prior to C–Cl bond cleavage, which in biological reactions are commonly related to extracellular and intracellular mass transfers or to enzyme-substrate binding [65-68]. For instance, the mass transfer of the substrate to the enzyme can be affected by extracellular processes such as dissolution, solubility, and transport to the cell or by intracellular factors like membrane barriers or sorption at the membranes or enzymes. These factors can impose rate limitations that mask the isotope effects [69,70]. Therefore, the $AKIE_C$ and $AKIE_{Cl}$ observed in our experiment cannot solely be attributed to the bond cleavage step, making it difficult to derive deeper mechanistic interpretation from them. Nevertheless, a further discussion was held based on previous studies.

The reductive dechlorination of the OCP DDT has been assumed to involve the substitution of an aliphatic Cl atom with a H atom through a single electron transfer mechanism, forming an alkyl radical as the first step of the reaction [71]. McGuire & Peters [72] suggested a similar

mechanism for the electrochemical reduction of MET. The $AKIE_C$ and $AKIE_{Cl}$ values obtained in the present experiment fall within the typical ranges for reductive dechlorination of a C-Cl bond ($AKIE_C$ =1.02 – 1.03, [58]) and are consistent with experimental ranges documented for the biotic reductive dechlorination of chlorinated volatile compounds ($AKIE_C$ =1.003 – 1.04 and $AKIE_{Cl}$ =1.003 – 1.015, [73-78]). Comparable AKIE values have been reported for the enzymatic reductive dechlorination of HCH isomers, assuming a stepwise dichloroelimination process (1.012 – 1.044 and 1.008 – 1.026, respectively) [79-81](Table A7). Finally, the obtained AKIE values are similar to those obtained by Heckel et al. [82] for single electron transfer reactions ($AKIE_C$ = 1.018, $AKIE_{Cl}$ = 1.008). Therefore, both AKIEs indicate that the first rate-limiting step of the reaction is the C−Cl bond cleavage. This is consistent with the transfer of a single electron as the first step, resulting in the removal of a Cl atom and the formation of an alkyl radical, which is subsequently protonated leading to DMDD (Fig. 3).

Considering the masking effect described above that limits mechanistic interpretation of AKIE values, the application of $AKIE_C$ versus $AKIE_{Cl}$ patterns, which cancels out rate limitations, was explored. Previous studies have suggested a relationship between $AKIE_C$ vs. $AKIE_{Cl}$ patterns and the mechanisms and/or the involved reductive dehalogenases involved in the dehalogenation of chlorinated volatile organic compounds [75,83]. While this discussion exceeds the scope of the present work due to limited data availability, this approach was explored for comparison with the limited AKIEs data on OCPs reductive dechlorination, particularly relating to the dichloroelimination of HCH isomers (Fig. A6). From this analysis, no definitive correlation can be inferred. However, since the obtained $AKIE_C$ vs. $AKIE_{Cl}$ ratio for MET falls closer to those of α-HCH, β-HCH, and γ-HCH than those of δ-HCH [79-81], the first rate-limiting step and/or the dehalogenase involved in MET reductive dechlorination in the present study may resemble the mechanisms observed for α-HCH, β-HCH, and γ-HCH, rather than those for δ-HCH. For HCHs, these discrepancies in AKIE values have been previously attributed to the mode of the bond cleavage depending on the position and/or orientation of the involved C-Cl bonds [81].

Under alkaline conditions, the dehydrochlorination of MET to MET-OLEF has been assumed to proceed via a nucleophilic elimination mechanism facilitated by hydroxyl ions in aqueous solution [27,84]. This mechanism involves the cleavage of both C-Cl and C-H bonds. The lack of C and Cl isotope fractionation in the alkaline hydrolysis experiment suggests a preferential cleavage of the C–H bond in the rate-limiting step. Additionally, any discernible C isotope fractionation is further reduced by a dilution effect due to the high number of C atoms in the molecule. A C-H bond cleavage as the rate-limiting step has similarly been proposed for the abiotic and enzymatic γ-HCH dehydrochlorination, as indicated by ME-CSIA [39,53,85]. In contrast to MET, a significant C isotope effect has been reported for HCH dehydrochlorination, which is likely attributed to a lower dilution effect since the HCH molecule contains only six C atoms, whereas the MET molecule has fifteen. We hypothesize that MET oxidation with base-activated PS also occurs by dehydrochlorination, similar to the oxidative dehydrochlorination of MET by ligninolytic enzymes [18]. This reaction involves the cleavage of the C-Cl bond and the elimination of a Cl radical [18]. The lack of C and Cl isotope fractionation in the PS experiment indicates again that the C-Cl bond cleavage was not the rate-determining step. In this sense, previous studies have demonstrated that the dehydrochlorination of DDT by $OH^{\bullet}$ or $SO_4^{\bullet-}$ radicals derived from peroxymonosulfate occurs with the attack of the radicals to the tertiary C atom located between the two rings of the DDT molecule as the first rate-limiting step [86]. Similarly, the decomposition of ozone under alkaline conditions [87] or the extracellular Fenton-like reaction utilized by brown-rot fungi [88] involves the attack of $OH^{\bullet}$ or $SO_4^{\bullet-}$ radicals to this tertiary C atom as the initial rate-limiting step. As a result, a stable tertiary radical is formed, which rapidly breaks down via homolysis of the C-Cl bond

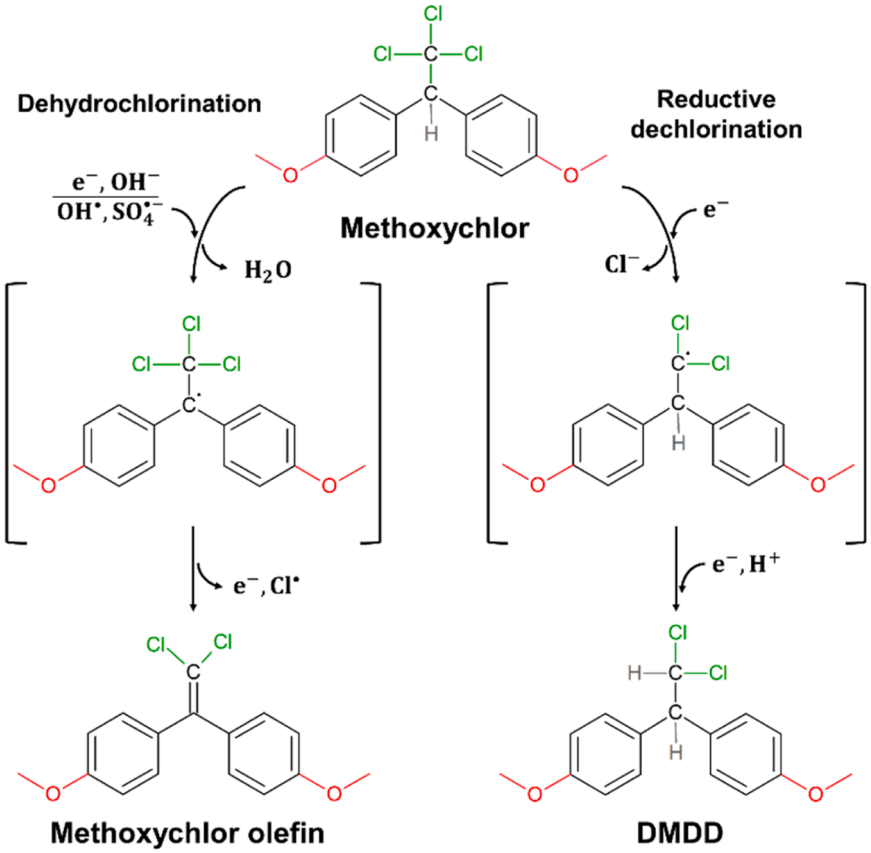

Fig. 3. Suggested degradation mechanisms for the dehydrochlorination (left) and the reductive dechlorination (right) of MET.

leading to the formation of a dehydrochlorinated product. A comparable mechanism to the one described for DDT oxidation is thus proposed for MET dehydrochlorination by both alkaline hydrolysis and oxidation with alkaline-activated PS (Fig. 3).

3.6. Changes in the bacterial community composition and diversity

In total, 744 OTUs were assigned through amplicon sequencing of the V3 and V4 variable regions of the 16S rRNA gene in slurry samples collected at the beginning (T0, 414 OTUs) and at the end (TF, 357 OTUs) of the biodegradation experiment. The overall taxonomic profile was classified in 28 phyla, 66 classes, 135 orders, 195 families and 273 genera. These taxonomies were distributed in 28 phyla, 59 classes, 117 orders, 169 families and 233 genera in the T0 sample. In contrast, in the TF slurry 23 phyla, 55 classes, 102 orders, 153 families and 209 genera were identified. The distribution and composition of the reported taxonomy gave a measure of alpha diversity within each sample (Table A8). The Margalef's specific diversity index suggested an environment with high diversity for each sample. The Pielou's evenness index, known as the ratio of observed diversity to the maximum expected diversity [89], showed in both cases values close to 1, corresponding to a situation where all species are equally abundant or to a medium-high dominance of a few species. The Shannon-Wiener index indicated a high species diversity in both samples [90]. At last, for both samples, the Simpson's index, which is strongly influenced by the importance of the most dominant species [90,91], indicated a high probability that two randomly chosen individuals in the community belong to the same group. Therefore, alpha diversity indexes indicated a high and similar degree of genetic richness and diversity in both slurry samples.

Despite of the variation in the distribution of the bacterial communities between the beginning and the end of the experiment, these changes did not greatly affect the overall community structure. At phylum level, both samples showed similar relative abundances of the mayor phyla, with similar representatives (Fig. A7). In the sample T0, phyla representing 80 % of the total relative abundance were dominated by Patescibacteria (30.6 %), Bacteroidota (16.9 %), Proteobacteria (11.7 %), Firmicutes (10.7 %) and Chloroflexi (10 %). Similarly, in the TF sample, these phyla – Patescibacteria (32.6 %), Bacteroidota (14.2 %), Chloroflexi (13.5 %), Proteobacteria (10.8 %) and Firmicutes (10 %) – accounted for 81 % of the total abundance. Therefore, from T0 to TF, the abundance of Patescibacteria and Chloroflexi slightly increased, while the phyla Bacteroidota, Proteobacteria and Firmicutes showed a tendency towards a decreased abundance.

At the family level, the global distribution of taxa exhibited consistent variation across samples (Fig. 4). Dojkabacteria and *Anaerolineaceae* were the dominant families in both samples, accounting for 17.8 % and 9.6 % of the total abundances in T0 and 20 % and 12.4 % in TF, respectively. In T0, these families together with *Synergistaceae* (3.9 %), Candidatus (Ca.) Falkowbacteria (3.7 %), and *Dysgonomonadaceae* (3.6 %) collectively represented 38.6 % of the relative abundance within the total community structure. In TF, the principal families were Dojkabacteria (20 %), *Anaerolineaceae* (12.4 %), *Dysgonomonadaceae* (4.9 %), Ca. Pacebacteria (4.2 %) and *Bacteroidetes* vadinHA17 (4.1 %), accounting for 45.6 % of the total bacterial distribution. In addition, Ca. Falkowbacteria, *Spirochaetaceae, Pseudomonadaceae, Williamwhitmaniaceae* and *Izemoplasmataceae* exhibited increased abundances from T0 to TF.

The families *Mycobacteriaceae and Bacillaceae* were suggested as possible mediators of MET dechlorination by Satsuma & Masuda [24]. In the presented experiment, the family *Mycobacteriaceae* was accounted for 0.30 % of the bacterial community in the T0 sample, which slightly increased to 0.37 % by the end of the experiment. In contrast, the family

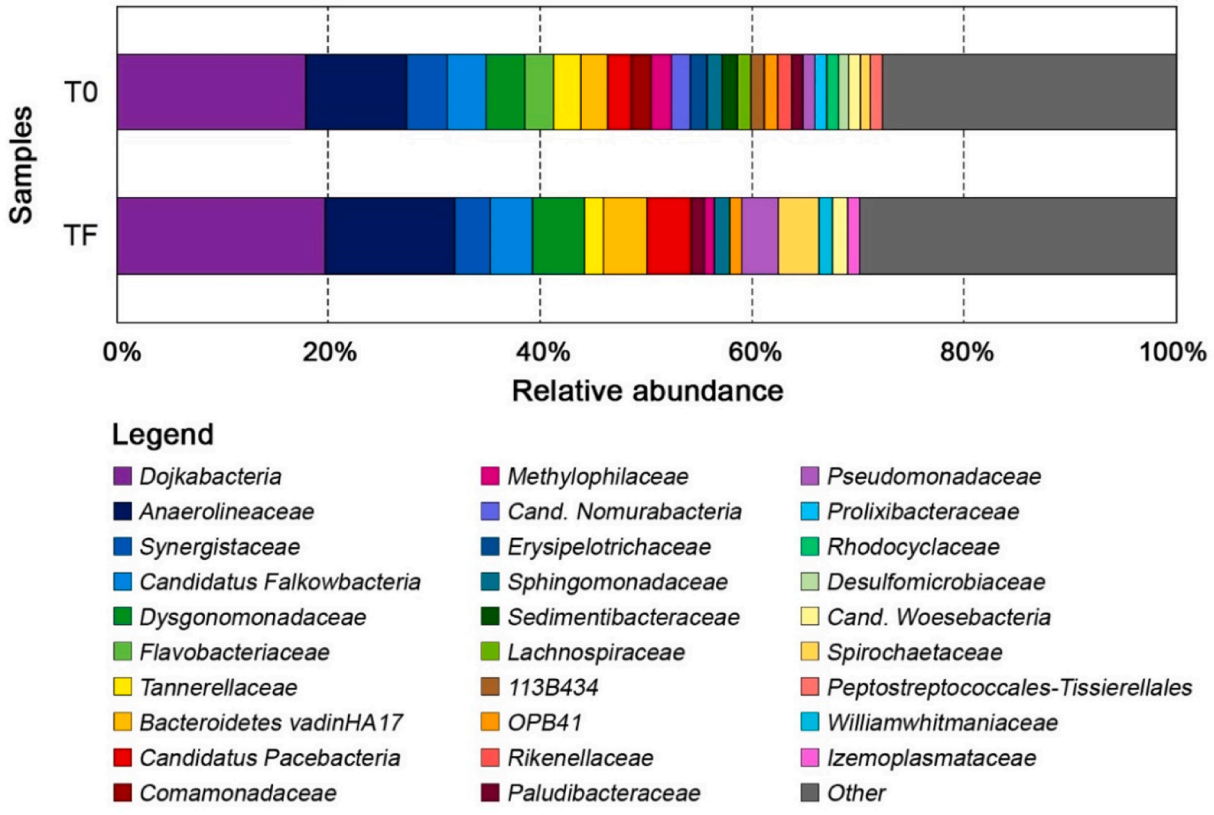

Fig. 4. Relative abundance (%) of the major families identified in the slurry samples of the biodegradation experiment. Only families with a relative abundance > 1 % of total bacteria population were considered.

Bacillaceae was only detected in T0 at very low relative abundance (<0.1 %). Other families previously reported as being involved in MET dechlorination, such as *Mycobacteriaceae*, *Moraxellaceae*, *Aeromonadaceae*, *Streptomycetaceae*, *Micromonosporaceae* and *Enterobacteriaceae* [23,25,26,24], were not detected in any of the samples, with the exception of a *Mycobacterium* (relative abundances of 0.3 % in both samples).

According to the results of previous anoxic microcosm experiments with slurry of this well performed ten years ago [76], well-known organohalide-respiring bacteria such as *Dehalococcoides*, *Geobacter*, *Dehalobacter* or *Dehalogenimonas* [92], were not found (when detected, corresponding families showed relative abundances below 0.1 %). This fact was attributed to inhibition effects by the presence of multiple contaminants in this site such as tetrachloromethane or chloroform [76].

The dominant Dojkabacteria (18 % in T0 and 20 % in TF), belonging to the phylum Patescibacteria, is a recently identified bacterial family discovered in the methanogenic zone of a hydrocarbon-contaminated aquifer, yet lacking any cultivated representatives [93]. Dojkabacteria can be associated to carbohydrate degradation or fermentative lifestyles [94,95]. The substantial phylogenetic divergence of Dojkabacteria and its closely related bacteria likely encompasses a wide range of biochemical and metabolic capabilities, many of which remain undiscovered. Recently, Dojkabacteria were found to be potentially involved in the dechlorination of the OCP chlordecone in microcosms constructed anaerobically from chlordecone-impacted soils [96]. Within the Chloroflexi phylum, members of the family *Anaerolineaceae*, whose relative abundance increase slightly from T0 (9.6 %) to TF (12.4 %) in the current experiments, have previously been associated with the reductive dechlorination of polychlorinated biphenyls in wetland sediments bioaugmented with a microbial consortium comprising the organohalide-respiring bacteria *Dehalococcoides* [97].

Previous studies indicated that members of the phyla Bacteroidota and Proteobacteria possess the ability to degrade OCPs [98]. Within Bacteroidota, the increased presence of *Dysgonomonadaceae* and *Bacteroidetes* vadinHA17 at the end of the biodegradation experiment may be attributed to this metabolic capacity. Indeed, members of *Dysgonomonadaceae* were previously detected in a high relative abundance in the slurry collected from this well ten years ago [76]. Similarly, members of the family *Pseudomonadaceae*, belonging to γ-Proteobacteria, may exhibit analogous metabolic activities. Members of *Pseudomonadaceae* are known to grow in the presence of MET and have also been implicated in the degradation of other organochlorine compounds, such as 2,4 dichlorobipheny [99] and the OCPs endrin, aldrin and DDT [100]. In fact, one of the most metabolically active genera in chlorinated methanes degradation in previous experiments with slurry of this well belonged to *Pseudomonadaceae* [76] Finally, members of *Spirochaetaceae* (phylum Spirochaetota), which showed a slight increase from T0 (1 %) to TF (3.6 %), were also previously detected in anoxic experiments with chlordecone degradation by a consortium enriched from a sludge from a wastewater treatment plant [101] and in anaerobic watersheds sediments contaminated with dieldrin and DDT [102].

Therefore, members of Dojkabacteria, *Anaerolineaceae*, *Dysgonomonadaceae*, *Bacteroidetes* vadinHA17, *Pseudomonadaceae* and *Spirochaetaceae* might have been involved in the reductive dechlorination of MET in the present experiment. According to our previous studies in this well [76], the slight changes in the community structure of the aquifer slurry from the beginning to the end of the experiment, alongside with the rapid MET degradation, indicate the presence of a well-established and adapted microbial community as well as favorable conditions in the aquifer for reductive dechlorination of chlorinated pollutants.

4. Conclusions

The degradation of MET through biotic reductive dechlorination, alkaline hydrolysis, and oxidation with alkaline-activated PS followed pseudo-first-order kinetics. DMDD was identified as the transformation product in the biotic reductive dechlorination process, while MET-OLEF was detected in the alkaline hydrolysis and oxidation with alkaline-activated PS processes. The changes in DMDD and MET-OLEF concentrations with time suggest a further degradation of the transformation products. Moreover, the higher water affinity of DMDD compared to MET resulted in a displacement of DMDD from the solid to the water phase during the biotic reductive dechlorination experiment. Decision-makers should consider that when biotic reductive dechlorination is occurring at MET-polluted sites, concentrations of DMDD in water may increase, thereby enhancing its mobility through the hydrological system.

Degradation by alkaline hydrolysis and oxidation with alkaline-activated PS resulted in insignificant C and Cl isotope fractionation. The absence of Cl isotope fractionation confirms that the rate-limiting step involve the cleavage of the C-H bond rather than the C-Cl bond. In contrast, biotic reductive dechlorination resulted in significant C and Cl isotope fractionation and the dual isotope slope ($\Lambda_{C/Cl} = 0.4 \pm 0.1$) and AKIEs values ($AKIE_C = 1.014 \pm 0.005$; $AKIE_C = 1.006 \pm 0.003$) were calculated. These results demonstrate that the initial step of the reductive dechlorination of MET involves the cleavage of the C-Cl bond, thereby distinguishing it from the dehydrochlorination process.

The results of the isotope analysis allow to differentiate between the reductive dechlorination of MET and its transformation through alkaline hydrolysis and oxidation with alkaline-activated PS. However, they do not allow to differentiate the two processes involving a dehydrochlorination pathway, namely the alkaline hydrolysis and the oxidation with alkaline-activated PS. Accordingly, future research should emphasize the implementation of hydrogen isotope analysis (δ^2H-CSIA), as it shows potential for distinguishing between these degradation processes where the rate-limiting step involves the cleavage of the C-H bond. However, these first reported isotopic fractionation values for MET can serve as benchmarks for future comparisons with C and Cl fractionation patterns in other transformation processes. This comparison could help to differentiate degradation pathways in field studies.

Finally, the families Dojkabacteria, *Anaerolineaceae, Dysgonomonadaceae*, *Bacteroidetes vadinHA17*, *Pseudomonadaceae*, and *Spirochaetaceae* exhibited notable increases in the relative abundance within the aquifer slurry throughout the biodegradation experiment. Consequently, these bacterial families emerge as strong candidates for participating in MET reductive dechlorination under strictly anoxic conditions. Further research should be conducted to specify the role of each family in the reductive dechlorination of MET under strictly anoxic conditions.

The current study advances the understanding of MET degradation by providing novel insights and perspective into the mechanisms involved in biotic reductive dechlorination, alkaline hydrolysis and oxidation with alkaline-activated PS processes. In addition, although further investigations are essential, the microbiological findings obtained from the strictly anoxic conditions experiment could significantly enhance our understanding of microbial behavior in MET-polluted aquifers. This knowledge holds promise for its application in bioremediation strategies. These outcomes could improve the monitoring of MET transformation processes at contaminated sites by utilizing established methods for performing C and Cl isotope analysis of environmental samples and at environmentally-relevant concentrations [50]. This information would provide decision-makers valuable insights into the fate of MET in natural environments, aiding in the determination and monitoring of optimal remediation strategies.

Environmental implications

As an organochlorine pesticide, methoxychlor poses a significant environmental issue due to its toxicity and bioaccumulation in the food chain, threatening the environment and human health. Understanding

its environmental behavior serves as a scientific foundation for risk avoidance and mitigation. In this research, isotopic analyses of methoxychlor have proven useful for differentiating between various degradation processes, offering new insights into their mechanisms. Microbiological findings enhance our understanding of methoxychlor biodegradation in aquifers. This information provides decision-makers with valuable insights into the behavior of methoxychlor and its transformation products in the environment, aiding the determination and monitoring of optimal remediation strategies.

CRediT authorship contribution statement

Martí Vinyes-Nadal: Writing – original draft, Visualization, Validation, Methodology, Investigation, Formal analysis, Data curation, Conceptualization. **Steffen Kümmel:** Writing – review & editing, Formal analysis. **Yolanda Espín:** Writing – review & editing, Methodology, Formal analysis. **Juan José Gómez-Alday:** Writing – review & editing, Resources, Project administration, Funding acquisition. **Matthias Gehre:** Resources. **Neus Otero:** Writing – review & editing, Supervision, Resources, Project administration, Funding acquisition. **Clara Torrentó:** Writing – review & editing, Writing – original draft, Supervision, Resources, Project administration, Funding acquisition, Data curation, Conceptualization.

Declaration of Competing Interest

The authors declare that they have no known competing financial interests or personal relationships that could have appeared to influence the work reported in this paper.

Data availability

Data will be made available on request.

Acknowledgements

This study was supported by PACE (CGL2017-87216-C4-1-R), REMECLOR (PDC2021-120861-C21), and PASITO (CNS2022-135543) projects, all funded by MICIU/AEI/10.13039/501100011033 and by European Union NextGenerationEU/PRTR. Funding was also received from the ADVANCE4WATER-ISOTRACE (PID2022-139911OB-C4-01) and ADVANCE4WATER-ATRAPA (PID2022-139911OB-C44) projects, funded by MICIU/AEI/10.13039/501100011033/FEDER,UE, the ANCOR-TECH (SBPLY/21/180501/000055) project, funded by the *Junta de Comunidades de Castilla-La Mancha*, and from the European Union's Horizon 2020 research and innovation programme under the Marie Sklodowska-Curie grant agreement No 837873. This work was also partly supported by the *Generalitat de Catalunya* through a Consolidate Research Group (2021SGR 00308). M. Vinyes Nadal received a PhD grant (FPU18/03862) from the "*Ayudas de Formación de Profesorado Universitario*" program of the Spanish Ministry of Universities and a small help for consumables from *Accions de Suport de l'Institut de Recerca de l'Aigua (IdRA) a la Recerca de Joves Investigadors* 2021, 2022 and 2023. The authors would like to thank the Technological Centers of the University of Barcelona (CCiT-UB) for the technical assistance. The authors are also thankful for the use of the analytical facilities of the Laboratories for Stable Isotopes (LSI) and the Centre for Chemical Microscopy (ProVIS) at UFZ Leipzig.

Appendix A. Supporting information

Supplementary data associated with this article can be found in the online version at doi:10.1016/j.jhazmat.2024.135929.

References

[1] Ntow, W.J., 2005. Pesticide residues in Volta lake, Ghana. Lakes Reserv: Res Manag 10 (4), 243–248.
[2] Swarcewicz, M.K., Gregorczyk, A., 2012. The effects of pesticide mixtures on degradation of pendimethalin in soils. Environ Monit Assess 184 (5), 3077–3084. https://doi.org/10.1007/s10661-011-2172-x.
[3] Xue, N., Zhang, D., Xu, X., 2006. Organochlorinated pesticide multiresidues in surface sediments from Beijing Guanting reservoir. Water Res 40 (2), 183–194. https://doi.org/10.1016/j.watres.2005.07.044.
[4] Basavarajappa, M.S., Craig, Z.R., Hernández-Ochoa, I., Paulose, T., Leslie, T.C., Flaws, J.A., 2011. Methoxychlor reduces estradiol levels by altering steroidogenesis and metabolism in mouse antral follicles in vitro. Toxicol Appl Pharmacol 253 (3), 161–169.
[5] Chen, G., 2014. Methoxychlor. Encyclopedia of Toxicology, Third Edition, pp. 254–255. https://doi.org/10.1016/B978-0-12-386454-3.00162-7.
[6] Harris, M.O., Miller, L.L., Little, S., McClure, P., Sutton, W., 2002. Toxicological profile for methoxychlor. ATSDR.
[7] ATSDR. (2022). *ATSDR's Substance Priority List*. ⟨https://www.atsdr.cdc.gov/spl/index.html#⟩.
[8] Stuchal, L.D., Kleinow, K.M., Stegeman, J.J., James, M.O., 2006. Demethylation of the pesticide methoxychlor in liver and intestine from untreated, methoxychlor-treated, and 3-methylcholanthrene-treated channel catfish (Ictalurus punctatus): evidence for roles of CYP1 and CYP3A family isozymes. Drug Metab Dispos 34 (6), 932–938.
[9] UN. (2019). Proposed for listing under the Stockholm Convention Methoxychlor (Issue 72).
[10] Affum, A.O., Acquaah, S.O., Osae, S.D., Kwaansa-Ansah, E.E., 2018. Distribution and risk assessment of banned and other current-use pesticides in surface and groundwaters consumed in an agricultural catchment dominated by cocoa crops in the Ankobra Basin, Ghana. Sci Total Environ 633, 630–640.
[11] Cruzeiro, C., Rocha, E., Pardal, M.Â., Rocha, M.J., 2016. Seasonal-spatial survey of pesticides in the most significant estuary of the Iberian Peninsula–the Tagus River estuary. J Clean Prod 126, 419–427.
[12] Prajapati, S., Challis, J.K., Jardine, T.D., Brinkmann, M., 2022. Levels of pesticides and trace metals in water, sediment, and fish of a large, agriculturally-dominated river. Chemosphere 308, 136236.
[13] Oyekunle, J.A.O., Adegunwa, A.O., Ore, O.T., 2022. Distribution, source apportionment and health risk assessment of organochlorine pesticides in drinking groundwater. Chem Afr 5 (4), 1115–1125.
[14] Thiombane, M., Petrik, A., Di Bonito, M., Albanese, S., Zuzolo, D., Cicchella, D., Lima, A., Qu, C., Qi, S., De Vivo, B., 2018. Status, sources and contamination levels of organochlorine pesticide residues in urban and agricultural areas: a preliminary review in central–southern Italian soils. Environ Sci Pollut Res 25, 26361–26382.
[15] Kim, J.-Y., Yi, B.-R., Go, R.-E., Hwang, K.-A., Nam, K.-H., Choi, K.-C., 2014. Methoxychlor and triclosan stimulates ovarian cancer growth by regulating cell cycle-and apoptosis-related genes via an estrogen receptor-dependent pathway. Environ Toxicol Pharmacol 37 (3), 1264–1274.
[16] Anderson, R.L., DeFoe, D.L., 1980. Toxicity and bioaccumulation of endrin and methoxychlor in aquatic invertebrates and fish. Environ Pollut Ser A Ecol Biol 22 (2), 111–121.
[17] Bourguignon, N., Fuentes, M.S., Benimeli, C.S., Cuozzo, S.A., Amoroso, M.J., 2014. Aerobic removal of methoxychlor by a native Streptomyces strain: identification of intermediate metabolites. Int Biodeterior Biodegrad 96, 80–86. https://doi.org/10.1016/j.ibiod.2014.09.016.
[18] Hirai, H., Nakanishi, S., Nishida, T., 2004. Oxidative dechlorination of methoxychlor by ligninolytic enzymes from white-rot fungi. Chemosphere 55 (4), 641–645. https://doi.org/10.1016/j.chemosphere.2003.11.035.
[19] Satsuma, K., Masuda, M., Sato, K., 2012. O-demethylation and successive oxidative dechlorination of methoxychlor by Bradyrhizobium sp.strain 17-4, isolated from river sediment. Appl Environ Microbiol 78 (15), 5313–5319. https://doi.org/10.1128/AEM.01180-12.
[20] Zepp, R.G., Wolfe, N.L., Gordon, J.A., Fincher, R.C., 1976. Light-induced transformations of methoxychlor in aquatic systems. J Agric Food Chem 24 (4), 727–733.
[21] Roberts, T.R., Hutson, D.H., Lee, P.W., Nicholls, P.H., Plimmer, J.R., Roberts, M. C., Croucher, L., 2007. Metabolic pathways of agrochemicals: part 1: herbicides and plant growth regulators. R Soc Chem.
[22] Muir, D.C.G., Yarechewski, A.L., 1984. Degradation of methoxychlor in sediments under various redox conditions. J Environ Sci Health Part B 19 (3), 271–295.
[23] Baarschers, W.H., Bharath, A.I., Elvish, J., Davies, M., 1982. The biodegradation of methoxychlor by Klebsiella pneumoniae. Can J Microbiol 28 (2), 176–179.
[24] Satsuma, K., Masuda, M., 2012. Reductive dechlorination of methoxychlor by bacterial species of environmental origin: Evidence for primary biodegradation of methoxychlor in submerged environments. J Agric Food Chem 60 (8), 2018–2023. https://doi.org/10.1021/jf2048614.
[25] Fuentes, M.S., Alvarez, A., Sáez, J.M., Benimeli, C.S., Amoroso, M.J., 2014. Methoxychlor bioremediation by defined consortium of environmental Streptomyces strains. Int J Environ Sci Technol 11, 1147–1156.
[26] Fuentes, M.S., Benimeli, C.S., Cuozzo, S.A., Amoroso, M.J., 2010. Isolation of pesticide-degrading actinomycetes from a contaminated site: bacterial growth, removal and dechlorination of organochlorine pesticides. Int Biodeterior Biodegrad 64 (6), 434–441.

[27] Wolfe, N.L., Zepp, R.G., Paris, D.F., Baughman, G.L., Hollis, R.C., 1977. Methoxychlor and DDT degradation in water: rates and products. Environ Sci Technol 11 (12), 1077–1081. https://doi.org/10.1021/es60135a003.
[28] Ribeiro, A.R., Nunes, O.C., Pereira, M.F.R., Silva, A.M.T., 2015. An overview on the advanced oxidation processes applied for the treatment of water pollutants defined in the recently launched Directive 2013/39/EU. Environ Int 75, 33–51. https://doi.org/10.1016/j.envint.2014.10.027.
[29] Chamberlain, E., Shi, H., Wang, T., Ma, Y., Fulmer, A., Adams, C., 2012. Comprehensive screening study of pesticide degradation via oxidation and hydrolysis. J Agric Food Chem 60 (1), 354–363. https://doi.org/10.1021/jf2033158.
[30] Jin, X., Peldszus, S., Huck, P.M., 2012. Reaction kinetics of selected micropollutants in ozonation and advanced oxidation processes. Water Res 46 (19), 6519–6530. https://doi.org/10.1016/j.watres.2012.09.026.
[31] Zaleska, A., Hupka, J., Wiergowski, M., Biziuk, M., 2000. Photocatalytic degradation of lindane, p,p′-DDT and methoxychlor in an aqueous environment. J Photochem Photobiol A: Chem 135 (2), 213–220. https://doi.org/10.1016/S1010-6030(00)00296-3.
[32] Huang, Y., Yang, Y., Wang, X., Yuan, X., Pi, N., Yuan, H., Liu, X., Ni, C., 2018. Heterogeneous Fenton-like degradation of methoxychlor in water using two different FeS@hydrotalcites (LHDs) and Fe3O4@LHDs catalysts prepared via an in situ growth method. Chem Eng J 342, 142–154. https://doi.org/10.1016/j.cej.2018.02.056.
[33] Zhou, Z., Liu, X., Sun, K., Lin, C., Ma, J., He, M., Ouyang, W., 2019. Persulfate-based advanced oxidation processes (AOPs) for organic-contaminated soil remediation: a review. Chem Eng J 372, 836–851.
[34] Checa-Fernández, A., Santos, A., Conte, L.O., Romero, A., Dominguez, C.M., 2022. Enhanced remediation of a real HCH-polluted soil by the synergetic alkaline and ultrasonic activation of persulfate. Chem Eng J 440, 135901.
[35] Checa-Fernández, A., Santos, A., Romero, A., Dominguez, C.M., 2021. Remediation of real soil polluted with hexachlorocyclohexanes (α-HCH and β-HCH) using combined thermal and alkaline activation of persulfate: optimization of the operating conditions. Sep Purif Technol 270, 118795.
[36] Zhu, C., Fang, G., Dionysiou, D.D., Liu, C., Gao, J., Qin, W., Zhou, D., 2016. Efficient transformation of DDTs with persulfate activation by zero-valent iron nanoparticles: a mechanistic study. J Hazard Mater 316, 232–241. https://doi.org/10.1016/j.jhazmat.2016.05.040.
[37] Zhu, C., Wang, D., Zhu, F., Liu, S., Fang, G., Gao, J., Zhou, D., 2021. Rapid DDTs degradation by thermally activated persulfate in soil under aerobic and anaerobic conditions: reductive radicals vs. oxidative radicals. J Hazard Mater 402, 123557. https://doi.org/10.1016/j.jhazmat.2020.123557.
[38] Wacławek, S., Silvestri, D., Hrabák, P., Padil, V.V.T., Torres-Mendieta, R., Wacławek, M., Černík, M., Dionysiou, D.D., 2019. Chemical oxidation and reduction of hexachlorocyclohexanes: a review. Water Res 162, 302–319. https://doi.org/10.1016/j.watres.2019.06.072.
[39] Kannath, S., Adamczyk, P., Wu, L., Richnow, H.H., Dybala-Defratyka, A., 2019. Can alkaline hydrolysis of γ-HCH serve as a model reaction to study its aerobic enzymatic dehydrochlorination by LinA? Int J Mol Sci 20 (23), 5955.
[40] Fenner, K., Canonica, S., Wackett, L.P., Elsner, M., 2013. Evaluating pesticide degradation in the environment: Blind spots and emerging opportunities. Science 341 (6147), 752–758. https://doi.org/10.1126/science.1236281.
[41] Elsner, M., Imfeld, G., 2016. Compound-specific isotope analysis (CSIA) of micropollutants in the environment - current developments and future challenges. Curr Opin Biotechnol 41 (Table 1), 60–72. https://doi.org/10.1016/j.copbio.2016.04.014.
[42] Hofstetter, T.B., Bakkour, R., Buchner, D., Eisenmann, H., Fischer, A., Gehre, M., Haderlein, S.B., Höhener, P., Hunkeler, D., Imfeld, G., 2024. Perspectives of compound-specific isotope analysis of organic contaminants for assessing environmental fate and managing chemical pollution. Nat Water 2 (1), 14–30. https://doi.org/10.1038/s44221-023-00176-4.
[43] Hofstetter, T.B., Schwarzenbach, R.P., Bernasconi, S.M., 2008. Assessing transformation processes of organic compounds using stable isotope fractionation. ACS Publications.
[44] Hunkeler, D., Meckenstock, R.U., Sherwood Lollar, B., Schmidt, T.C., Wilson, J.T., Schmidt, T., Wilson, J., 2008. A guide for assessing biodegradation and source identification of organic ground water contaminants using compound specific isotope analysis (CSIA). US EPA, *Ada*.
[45] Elsner, M., 2010. Stable isotope fractionation to investigate natural transformation mechanisms of organic contaminants: principles, prospects and limitations. J Environ Monit 12 (11), 2005–2031.
[46] Elsner, M., Jochmann, M.A., Hofstetter, T.B., Hunkeler, D., Bernstein, A., Schmidt, T.C., Schimmelmann, A., 2012. Current challenges in compound-specific stable isotope analysis of environmental organic contaminants. Anal Bioanal Chem 403, 2471–2491.
[47] Hofstetter, T.B., Berg, M., 2011. Assessing transformation processes of organic contaminants by compound-specific stable isotope analysis. TrAC Trends Anal Chem 30 (4), 618–627.
[48] Blessing, M., Baran, N., 2022. A review on environmental isotope analysis of aquatic micropollutants: recent advances, pitfalls and perspectives. TrAC Trends Anal Chem, 116730.
[49] Höhener, P., Guers, D., Malleret, L., Boukaroum, O., Martin-Laurent, F., Masbou, J., Payraudeau, S., Imfeld, G., 2022. Multi-elemental compound-specific isotope analysis of pesticides for source identification and monitoring of degradation in soil: a review. Environ Chem Lett 20 (6), 3927–3942.
[50] Vinyes-Nadal, M., Masbou, J., Kümmel, S., Gehre, M., Imfeld, G., Otero, N., Torrentó, C., 2024. Novel extraction methods and compound-specific isotope analysis of methoxychlor in environmental water and aquifer slurry samples. Sci Total Environ 931 (March). https://doi.org/10.1016/j.scitotenv.2024.172858.
[51] Lihl, C., Heckel, B., Grzybkowska, A., Dybala-Defratyka, A., Ponsin, V., Torrentó, C., Hunkeler, D., Elsner, M., 2020. Compound-specific chlorine isotope fractionation in biodegradation of atrazine. Environ Sci.
[52] Torrentó, C., Ponsin, V., Lihl, C., Hofstetter, T.B., Baran, N., Elsner, M., Hunkeler, D., 2021. Triple-element compound-specific stable isotope analysis (3D-CSIA): added value of Cl isotope ratios to assess herbicide degradation. Environ Sci Technol 55 (20), 13891–13901. https://doi.org/10.1021/acs.est.1c03981.
[53] Liu, Y., Fu, J., Wu, L., Kümmel, S., Nijenhuis, I., Richnow, H.H., 2022. Characterization of hexachlorocyclohexane isomer dehydrochlorination by LinA1 and LinA2 using multi-element compound-specific stable isotope analysis. Environ Sci Technol 56 (23), 16848–16856.
[54] Rodríguez-Fernández, D., Torrentó, C., Palau, J., Marchesi, M., Soler, A., Hunkeler, D., Domènech, C., Rosell, M., 2018. Unravelling long-term source removal effects and chlorinated methanes natural attenuation processes by C and Cl stable isotopic patterns at a complex field site. Sci Total Environ 645, 286–296. https://doi.org/10.1016/j.scitotenv.2018.07.130.
[55] Kennedy, P., Kennedy, H., & Papadimitriou, S. (2005). The effect of acidification on the determination of organic carbon, total nitrogen and their stable isotopic composition in algae and marine sediment. *Rapid Communications in Mass Spectrometry: An International Journal Devoted to the Rapid Dissemination of Up-to-the-Minute Research in Mass Spectrometry*, *19*(8), 1063–1068.
[56] Droz, B., Drouin, G., Maurer, L., Villette, C., Payraudeau, S., Imfeld, G., 2021. Phase transfer and biodegradation of pesticides in water-sediment systems explored by compound-specific isotope analysis and conceptual modeling. Environ Sci Technol 55 (8), 4720–4728. https://doi.org/10.1021/acs.est.0c06283.
[57] Ojeda, A.S., Phillips, E., Mancini, S.A., Lollar, B.S., 2019. Sources of uncertainty in biotransformation mechanistic interpretations and remediation studies using CSIA. Anal Chem 91 (14), 9147–9153.
[58] Elsner, M., Zwank, L., Hunkeler, D., Schwarzenbach, R.P., 2005. A new concept linking observable stable isotope fractionation to transformation pathways of organic pollutants. Environ Sci Technol 39 (18), 6896–6916.
[59] Aeppli, C., Hofstetter, T.B., Amaral, H.I.F., Kipfer, R., Schwarzenbach, R.P., Berg, M., 2010. Quantifying in situ transformation rates of chlorinated ethenes by combining compound-specific stable isotope analysis, groundwater dating, and carbon isotope mass balances. Environ Sci Technol 44 (10), 3705–3711. https://doi.org/10.1021/es903895b.
[60] Hunkeler, D., Aravena, R., Butler, B.J., 1999. Monitoring microbial dechlorination of tetrachloroethene (PCE) in groundwater using compound-specific stable carbon isotope ratios: microcosm and field studies. Environ Sci Technol 33 (16), 2733–2738. https://doi.org/10.1021/es981282u.
[61] Bolyen, E., Rideout, J.R., Dillon, M.R., Bokulich, N.A., Abnet, C.C., Al-Ghalith, G.A., Alexander, H., Alm, E.J., Arumugam, M., Asnicar, F., 2019. Reproducible, interactive, scalable and extensible microbiome data science using QIIME 2. Nat Biotechnol 37 (8), 852–857.
[62] Callahan, B.J., McMurdie, P.J., Rosen, M.J., Han, A.W., Johnson, A.J.A., Holmes, S.P., 2016. DADA2: high-resolution sample inference from Illumina amplicon data. Nat Methods 13 (7), 581–583.
[63] Wang, Q., Garrity, G.M., Tiedje, J.M., Cole, J.R., 2007. Naive Bayesian classifier for rapid assignment of rRNA sequences into the new bacterial taxonomy. Appl Environ Microbiol 73 (16), 5261–5267.
[64] Pruesse, E., Quast, C., Knittel, K., Fuchs, B.M., Ludwig, W., Peplies, J., Glöckner, F.O., 2007. SILVA: a comprehensive online resource for quality checked and aligned ribosomal RNA sequence data compatible with ARB. Nucleic Acids Res 35 (21), 7188–7196.
[65] Cichocka, D., Siegert, M., Imfeld, G., Andert, J., Beck, K., Diekert, G., Richnow, H.-H., Nijenhuis, I., 2007. Factors controlling the carbon isotope fractionation of tetra-and trichloroethene during reductive dechlorination by Sulfurospirillum ssp. and Desulfitobacterium sp. strain PCE-S. FEMS Microbiol Ecol 62 (1), 98–107.
[66] Nijenhuis, I., Andert, J., Beck, K., Kästner, M., Diekert, G., Richnow, H.-H., 2005. Stable isotope fractionation of tetrachloroethene during reductive dechlorination by Sulfurospirillum multivorans and Desulfitobacterium sp. strain PCE-S and abiotic reactions with cyanocobalamin. Appl Environ Microbiol 71 (7), 3413–3419.
[67] Renpenning, J., Rapp, I., Nijenhuis, I., 2015. Substrate hydrophobicity and cell composition influence the extent of rate limitation and masking of isotope fractionation during microbial reductive dehalogenation of chlorinated ethenes. Environ Sci Technol 49 (7), 4293–4301.
[68] Thullner, M., Fischer, A., Richnow, H.-H., Wick, L.Y., 2013. Influence of mass transfer on stable isotope fractionation. Appl Microbiol Biotechnol 97, 441–452.
[69] Aelion, C.M., Höhener, P., Hunkeler, D., Aravena, R., 2009. Environmental isotopes in biodegradation and bioremediation. CRC Press.
[70] Nijenhuis, I., Richnow, H.H., 2016. Stable isotope fractionation concepts for characterizing biotransformation of organohalides. Curr Opin Biotechnol 41, 108–113.
[71] Foght, J., April, T., Biggar, K., Aislabie, J., 2001. Bioremediation of DDT-contaminated soils: a review. Biorernediation J 5 (3), 225–246.
[72] McGuire, C.M., Peters, D.G., 2016. Direct Electrochemical Reduction of 4, 4′-(2, 2, 2-Trichloroethane-1, 1-diyl) bis (methoxybenzene)(Methoxychlor) at Carbon and Silver Cathodes in Dimethylformamide. J Electrochem Soc 163 (5), G44.
[73] Franke, S., Seidel, K., Adrian, L., Nijenhuis, I., 2020. Dual element (C/Cl) isotope analysis indicates distinct mechanisms of reductive dehalogenation of chlorinated

ethenes and dichloroethane in Dehalococcoides mccartyi strain BTF08 with defined reductive dehalogenase inventories. Front Microbiol 11, 1507.
[74] Heckel, B., Phillips, E., Edwards, E., Sherwood Lollar, B., Elsner, M., Manefield, M.J., Lee, M., 2019. Reductive dehalogenation of trichloromethane by two different dehalobacter restrictus strains reveal opposing dual element isotope effects. Environ Sci Technol 53 (5), 2332–2343. https://doi.org/10.1021/acs.est.8b03717.
[75] Phillips, E., Bulka, O., Picott, K., Kümmel, S., Edwards, E.A., Nijenhuis, I., Gehre, M., Dworatzek, S., Webb, J., Sherwood Lollar, B., 2022. Investigation of active site amino acid influence on carbon and chlorine isotope fractionation during reductive dechlorination. FEMS Microbiol Ecol 98 (8), fiac072.
[76] Rodríguez-Fernández, D., Torrentó, C., Guivernau, M., Viñas, M., Hunkeler, D., Soler, A., Domènech, C., Rosell, M., 2018. Vitamin B12 effects on chlorinated methanes-degrading microcosms: dual isotope and metabolically active microbial populations assessment. Sci Total Environ 621, 1615–1625. https://doi.org/10.1016/j.scitotenv.2017.10.067.
[77] Soder-Walz, J.M., Torrentó, C., Algora, C., Wasmund, K., Cortés, P., Soler, A., Vicent, T., Rosell, M., Marco-Urrea, E., 2022. Trichloromethane dechlorination by a novel Dehalobacter sp. strain 8M reveals a third contrasting C and Cl isotope fractionation pattern within this genus. Sci Total Environ 813, 152659. https://doi.org/10.1016/j.scitotenv.2021.152659.
[78] Torrentó, C., Palau, J., Rodríguez-Fernández, D., Heckel, B., Meyer, A., Domènech, C., Rosell, M., Soler, A., Elsner, M., Hunkeler, D., 2017. Carbon and chlorine isotope fractionation patterns associated with different engineered chloroform transformation reactions. Environ Sci Technol 51 (11), 6174–6184. https://doi.org/10.1021/acs.est.7b00679.
[79] Liu, Y., Kümmel, S., Yao, J., Nijenhuis, I., Richnow, H.-H., 2020. Dual C–Cl isotope analysis for characterizing the anaerobic transformation of α, β, γ, and δ-hexachlorocyclohexane in contaminated aquifers. Water Res 184, 116128.
[80] Liu, Y., Liu, J., Renpenning, J., Nijenhuis, I., Richnow, H.-H., 2020. Dual C–Cl isotope analysis for characterizing the reductive dechlorination of α-and γ-hexachlorocyclohexane by two Dehalococcoides mccartyi strains and an enrichment culture. Environ Sci Technol 54 (12), 7250–7260.
[81] Zhang, X., Zheng, Y., Su, Z., Wang, Z., Zhang, J., Jia, Z., Kümmel, S., Qin, C., Liu, Y., Wang, S., 2024. Anaerobic biotransformation of hexachlorocyclohexane isomers in aqueous condition: dual C-Cl isotope fractionation and impact on microbial community compositions. Water Res, 121389.
[82] Heckel, B., Cretnik, S., Kliegman, S., Shouakar-Stash, O., McNeill, K., Elsner, M., 2017. Reductive outer-sphere single electron transfer is an exception rather than the rule in natural and engineered chlorinated ethene dehalogenation. Environ Sci Technol 51 (17), 9663–9673. https://doi.org/10.1021/acs.est.7b01447.
[83] Trueba-Santiso, A., Torrentó, C., Soder-Walz, J.M., Fernández-Verdejo, D., Rosell, M., Marco-Urrea, E., 2024. Dual C–Cl isotope fractionation offers potential to assess biodegradation of 1, 2-dichloropropane and 1, 2, 3-trichloropropane by Dehalogenimonas cultures. Chemosphere 358, 142170.
[84] Larson, R. (2018). Reaction mechanisms in environmental organic chemistry. Routledge.
[85] Schilling, I.E., Bopp, C.E., Lal, R., Kohler, H.-P.E., Hofstetter, T.B., 2019. Assessing aerobic biotransformation of hexachlorocyclohexane isomers by compound-specific isotope analysis. Environ Sci Technol 53 (13), 7419–7431. https://doi.org/10.1021/acs.est.9b01007.
[86] Qin, W., Fang, G., Wang, Y., Wu, T., Zhu, C., Zhou, D., 2016. Efficient transformation of DDT by peroxymonosulfate activated with cobalt in aqueous systems: Kinetics, products, and reactive species identification. Chemosphere 148, 68–76. https://doi.org/10.1016/j.chemosphere.2016.01.020.
[87] Balawejder, M., Antos, P., Czyjt-Kuryło, S., Józefczyk, R., Pieniążek, M., 2014. A novel method for degradation of DDT in contaminated soil. Ozone: Sci Eng 36 (2), 166–173.
[88] Purnomo, A.S., Kamei, I., Kondo, R., 2008. Degradation of 1,1,1-trichloro-2,2-bis (4-chlorophenyl) ethane (DDT) by brown-rot fungi. J Biosci Bioeng 105 (6), 614–621. https://doi.org/10.1263/jbb.105.614.
[89] Magurran, A.E., 1988. Diversity indices and species abundance models. Ecol Divers Meas 7–45.
[90] Heip, C.H.R., Herman, P.M.J., Soetaert, K., 1998. Indices of diversity and evenness. Oceanis 24 (4), 61–88.
[91] Simpson, E.H., 1949. Measurement of diversity. Nature 163 (4148), 688.
[92] Adrian, L., Löffler, F.E., 2016. Organohalide-respiring bacteria, Vol. 85. Springer.
[93] Dojka, M.A., Harris, J.K., Pace, N.R., 2000. Expanding the known diversity and environmental distribution of an uncultured phylogenetic division of bacteria. Appl Environ Microbiol 66 (4), 1617–1621.
[94] Campanaro, S., Treu, L., Rodriguez-R, L.M., Kovalovszki, A., Ziels, R.M., Maus, I., Zhu, X., Kougias, P.G., Basile, A., Luo, G., 2020. New insights from the biogas microbiome by comprehensive genome-resolved metagenomics of nearly 1600 species originating from multiple anaerobic digesters. Biotechnol Biofuels 13, 1–18.
[95] Speth, D.R., in't Zandt, M.H., Guerrero-Cruz, S., Dutilh, B.E., Jetten, M.S.M., 2016. Genome-based microbial ecology of anammox granules in a full-scale wastewater treatment system. Nat Commun 7 (1), 11172.
[96] Lomheim, L., Laquitaine, L., Rambinaising, S., Flick, R., Starostine, A., Jean-Marius, C., Edwards, E.A., Gaspard, S., 2020. Evidence for extensive anaerobic dechlorination and transformation of the pesticide chlordecone (C10Cl10O) by indigenous microbes in microcosms from Guadeloupe soil. PLoS One 15 (4), e0231219.
[97] Chen, C., Xu, G., Rogers, M.J., He, J., 2024. Metabolic synergy of dehalococcoides populations leading to greater reductive dechlorination of polychlorinated biphenyls. Environ Sci Technol 58 (5), 2384–2392. https://doi.org/10.1021/acs.est.3c08473.
[98] Kumar, M., Yadav, A.N., Saxena, R., Paul, D., Tomar, R.S., 2021. Biodiversity of pesticides degrading microbial communities and their environmental impact. Biocatal Agric Biotechnol 31, 101883.
[99] Jayanna, S.K., Gayathri, D., 2015. Degradation of 2, 4 dichlorobiphenyl via meta-cleavage pathway by Pseudomonas spp. consortium. Curr Microbiol 70, 871–876.
[100] Patil, K.C., Matsumura, F., Boush, G.M., 1970. Degradation of endrin, aldrin, and DDT by soil microorganisms. Appl Microbiol 19 (5), 879–881.
[101] Hellal, J., Saaidi, P.-L., Bristeau, S., Crampon, M., Muselet, D., Della-Negra, O., Mauffret, A., Mouvet, C., Joulian, C., 2021. Microbial transformation of chlordecone and two transformation products formed during in situ chemical reduction. Front Microbiol 12, 742039.
[102] Fiard, M., Militon, C., Sylvi, L., Migeot, J., Michaud, E., Jézéquel, R., Gilbert, F., Bihannic, I., Devesa, J., Dirberg, G., 2024. Uncovering potential mangrove microbial bioindicators to assess urban and agricultural pressures on Martinique island in the eastern Caribbean Sea. Sci Total Environ 928, 172217.